Finite Element Analysis of ECAP, TCAP, RUE and CGP Processes

IOP Conf. Series: Materials Science and Engineering **114** (2016) 012007 doi:10.1088/1757-899X/114/1/012007

Finite Element Analysis of ECAP, TCAP, RUE and CGP Processes

Deepak C Patil [1], Vinayak Kallannavar [1], Prabhakar M. Bhovi[2], S A Kori[3], K Venkateswarlu[4]

[1] KLE Dr. M. S. Sheshgiri College of Engineering and Technology, Udyambag, Belagavi-590008, India
[2] B. V. Bhoomaraddi College of Engineering and Technology, Hubballi-580031, India
[3] Basaveshwar Engineering College, Bagalkot-587102, Karnataka, India
[4] CSIR-National Aerospace Laboratories, Bangalore-560017, Karnataka, India

E-mail: todeepakpatil@rediffmail.com

Abstract. A finite element method was applied to study the various severe plastic deformation processes like, Equal Channel Angular Pressing (ECAP), Tubular Channel Angular Pressing (TCAP), Repetitive Upsetting and Extrusion (RUE) and Constrained Groove Pressing (CGP), considering aluminum AA-390 alloy as specimen material for all these processes. FEA simulation was carried out using AFDEX simulation tool. Effect of the various ECAP process parameters like, die corner angle, channel angle, and the coefficient of friction were analyzed. The die corner angles were divided into 2 equal parts for increasing the effectiveness of ECAP process, thereby increasing the channel number from 2 to 3 and further, their influence on ECAP process was investigated. A 3D simulation of TCAP was carried out for die shapes like triangular and trapezoidal, and variation of the generated stress and strain was plotted. In CGP, four cycle operation was carried out; wherein each cycle is composed of corrugating the specimen and subsequent straightening to original dimension. During RUE process, a maximum effective stress of 683.1 MPa was induced in the specimen after processing it for four complete cycles of RUE process; whereas the maximum strain induced during the same condition was 3.715.

1. Introduction

There has been considerable interest in recent years in enhancing material properties, through procedures involving the imposition of Severe Plastic Deformation (SPD). SPD processes impart large amount of strain in material without altering its cross section, and they permit variable strain paths which give rise to refined grain size. According to Hall-Petch relation, strength of materials increase with reduction in grain size. Usually the ultrafine grained materials are produced by top-down approach, as the materials produced by bottom-up approach will have porous structures. The grain refined material exhibit superior strength, ductility, high wear resistance, enhanced fatigue life, high corrosion resistance and high hardness. The commonly used SPD techniques suitable for bulk materials are High Pressure Torsion (HPT), Equal Channel Angular Pressing (ECAP), Cyclic Extrusion and Compression (CEC), Simple Shear Extrusion (SSE), and Torsional Extrusion (TE) etc. and Accumulative Roll Bonding (ARB), Repetitive Corrugation and Straightening (RCS), Constrained Groove Pressing (CGP) etc. for sheet materials.
Segal et al. [1] developed ECAP process as an effective tool to impose large plastic strains. Here the material with circular or square cross section is pressed through a die containing two channels of equal cross section as shown in Fig. 1, which causes simple shear deformation of material. Strain accumulated after N passes of ECAP process according to Segal et al. [Ψ=0], Iwashashi et al. and Goforth et al. are listed below [2],

$$\varepsilon = \frac{2N}{\sqrt{3}} \cot\left(\frac{\Psi}{2}\right)$$

$$\varepsilon = \frac{N}{\sqrt{3}}\left[2\cot\left(\frac{\Phi}{2}+\frac{\Psi}{2}\right)+\Psi\,\mathrm{cosec}\left(\frac{\Phi}{2}+\frac{\Psi}{2}\right)\right]$$

$$\varepsilon = \frac{N}{\sqrt{3}}\left[2\cot\left(\frac{\Phi}{2}+\frac{\Psi}{2}\right)+\Psi\right]$$

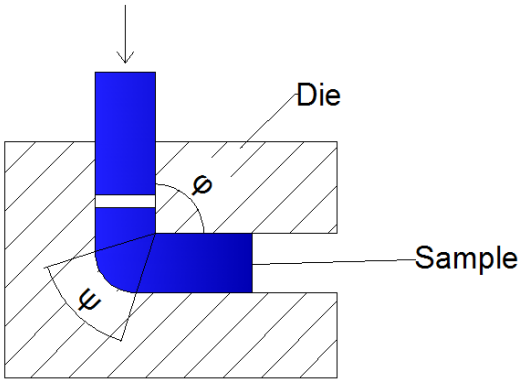

Fig. 1 Two dimensional schematic view of ECAP process

The important factors which influence ECAP process such as, die corner angle (Ψ), channel angle (Φ), processing routes (A, B_A, B_C, and C), pressing speed, working temperature, friction, number of passes etc. have been analyzed by many researchers, using both experimental and FEM methods for different metals and alloys [2-10].
Faraji et al. developed a high strain processing technique called TCAP process for tubes [11-13]. The tube constrained between inner and outer dies is pressed in to tubular angular channel by a hollow cylindrical punch as shown in Fig. 2. Two and three forming zones are observed in one cycle for triangular and trapezoidal shaped TCAP dies, which include channel angles (Φ_i) and corner angles (Ψ_i).

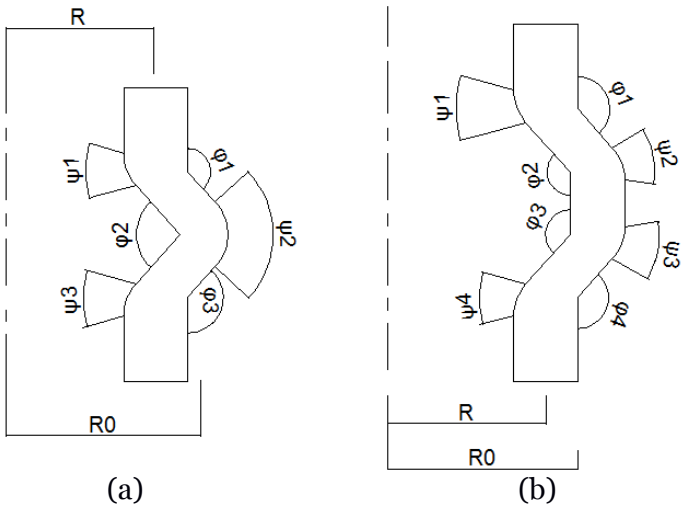

Fig. 2 Two dimensional schematic view of TCAP die
(a) triangular channel and (b) trapezoidal channel

The strain values for different geometry considering curvature angles as zero (Ψ_i=0) are given by [13],

$$\varepsilon = \sum_{i=1}^{4}\left[\frac{2\cot\left(\frac{\alpha}{2}\right)}{\sqrt{3}}\right] + \frac{4}{\sqrt{3}}\ln\frac{R}{R_o}$$ Trapezoidal channel

$$\varepsilon = \sum_{i=1}^{3}\left[\frac{2\cot\left(\frac{\alpha}{2}\right)}{\sqrt{3}}\right] + \frac{4}{\sqrt{3}}\ln\frac{R}{R_o}$$ Triangular channel

A typical RUE process consists of 2 basic steps (i) upsetting and (ii) extrusion as shown in Fig. 3. RUE process was developed by Aizawa et al. to process powder materials, in recent years extensive work has been done to extend the RUE process even to the bulk materials [14-16]. Work piece of cylindrical shape of known dimension is first subjected to upsetting then the upset work piece is subsequently subjected to extrusion, and the cycle continuous. During this, there will be variation in length and cross sectional area of specimen, depending on the process being carried out.

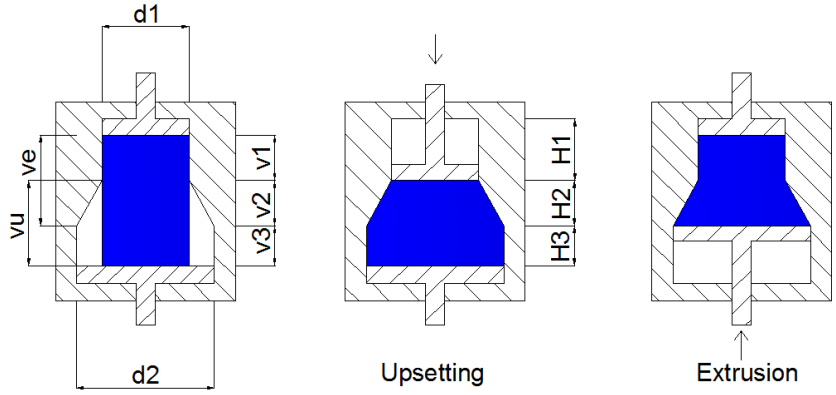

Fig. 3 Schematic view of RUE process showing load steps

The die is divided in to 3 regions with volumes V_1, V_2 and V_3, and the die is designed without violating the following constraints

$$V_1 + V_2 = V_2 + V_3$$

$$V_u = V_1 + V_2$$

$$V_e = V_2 + V_3$$

$$V_w = V_2 + V_3 = V_1 + V_2 = V_u + V_e$$

Where, V_u is Volume filled during upsetting stage, V_e is Volume filled during extrusion stage, and V_w is Volume of work piece.

For the first time Shin DH et al. [16] successfully presented the CGP process for sheet metals. Here the material is subjected to large amount of shear deformation with grooving and flattening dies respectively, as shown in Fig. 4. In the first stage the material is pressed between two grooved dies, in the second stage the deformed material is flattened by the flat dies. At the third stage the material is shifted to left or right by one groove length (t), and then the material is processed in stage 1 and then in stage 2.

Effective strain induced in CGP process is given by [17],

$$\varepsilon_{eff} = \sqrt{4\frac{\varepsilon_{xy}^{\ 2}}{3}}$$

$$\varepsilon_{xy} = \frac{\gamma_{xy}}{2}$$

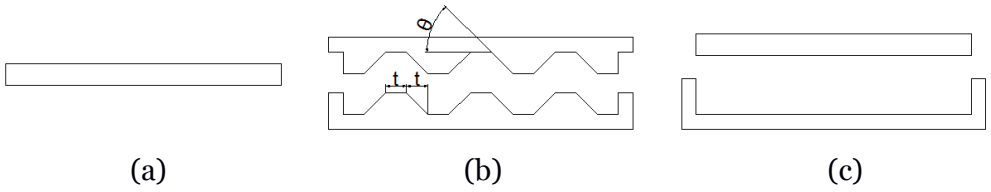

Fig. 4 Schematic view of CGP process showing (a) specimen, (b) grooving die, and (c) flattening die

Lot of work has been done to analyze the CGP process by both experimental and FEA techniques for different materials [17-23].

2. Finite Element Analysis

Finite element analysis is carried out using AFDEX simulation tool. For ECAP process, specimen with dimensions of 50 mm × 20 mm is used for processing. The ECAP die consists of 2 equal channels through which the material will be processed, where the channels are having same cross sectional dimensions as that of the specimen (diameter or width). The value of coefficient of friction at the die-specimen interface is considered as 0.20, and the punch moves with the velocity of 1 mm/second during the process. The specimen is divided to get ~4000 elements during the simulation.
Cylindrical tube with internal diameter of 7.5 mm, thickness of 2.5 mm and 45 mm long is considered for the analysis of the TCAP process. The value of R/R_o is fixed to 1.4, in both shapes of the dies i.e. triangular, and trapezoidal. The other dimensional parameters of TCAP dies are listed in Table 1. The tubes are processed at the velocity of 5 mm/minute and the coefficient of friction of 0.05 is considered for the contacts between die and specimen material. The material is segmented into ~40000 numbers of elements.

Table 1. Boundary conditions used for TCAP die

Channel Shapes	Φ_1	Φ_2	Φ_3	Φ_4	Ψ_1	Ψ_2	Ψ_3	Ψ_4
Triangular	135	90	135	-	0	90	0	-
Trapezoidal	135	135	135	135	0	0	0	0

For RUE process, specimen with dimension 32 mm × 10 mm is used for simulation. The die dimensions H1, H2 and H3 are considered as 7 mm, 11 mm and 14.5 mm respectively, and d1, d2 value are fixed to 28.3 mm and 20 mm. Radius of curvature of 10 mm is provided at the sharp corners to avoid folding defects. Both upsetting and extrusion processes are carried out at constant die speed of 1 mm/second and friction coefficient of 0.05 is provided at die-specimen interaction zones. Material is meshed to get ~4000 numbers of elements.
In CGP process, material of 65 mm long and 5 mm thick is analyzed. For grooved die the values of 't' and 'θ' are considered as 5 mm and 45°. The metal strip is segmented in to ~4000 number of elements for simulation. Process is carried out with die speed of 1 mm/second in all stages of process and friction coefficient of 0.1 is considered.
Aluminum AA-390 alloy is used as the specimen material for all the processes. The flow curve for Aluminum AA-390 is plotted in Fig. 5 and its material properties are listed in Table 2. Room temperature and the initial strain rate are considered as 25°C and 0.0001 per second.

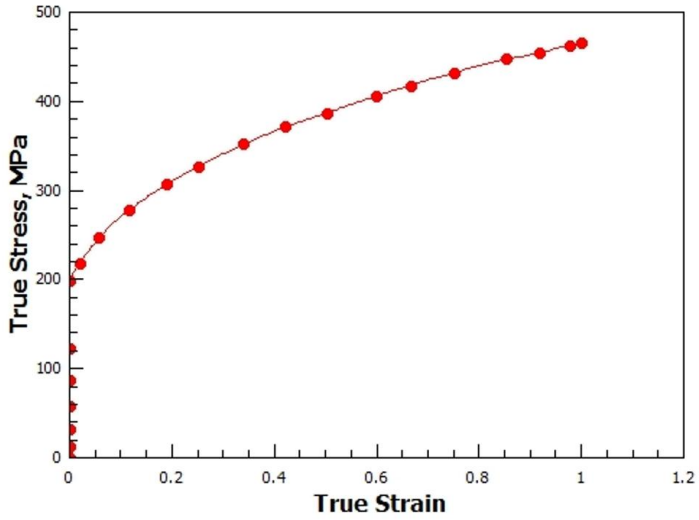

Fig. 5 Flow curve for aluminium AA-390

Table 2. Material properties for Aluminium AA-390 alloy

Young's Modulus (MPa)	69000
Poisson's Ratio	0.33
Density (kg/m^3)	2710
Coefficient of Thermal Expansion	0.0000235

Plastic flow of the material follows the equation given below,

$$\bar{\sigma} = Y_0 \left[1 + \frac{\bar{\varepsilon}}{b}\right]^a$$

Where,
Y_o= Minimum yield strength= 200 MPa
a= Strain hardening exponent= 0.28287
b= Strain reduction ratio= 0.05239

3. Results and discussion

Effect of friction on ECAP process is analyzed for, die corner angle (Ψ) and channel angle (Φ) of 90° each. Fig. 6 shows effective strain distribution of sample material processed by ECAP process, for different values of coefficient of friction viz. 0, 0.1, 0.2, 0.25, and 0.3. It can be seen that effective strain increases with increase in friction values, strain value reaches up to 1.603 when the value of coefficient of friction is increased to 0.3. Three different regions can be observed from ECAPed materials plotted in Fig. 6; (i) the front portion, where the magnitude of stains are nearly zero (ii) uniform strain distribution exist in the middle region, and (iii) at the junction of two channels, where the stain rate is maximum. It is also observed that the load requirement for the process increases with increasing magnitude of friction. Detailed results for ECAP process for different values of coefficient of friction are listed in Table 3.

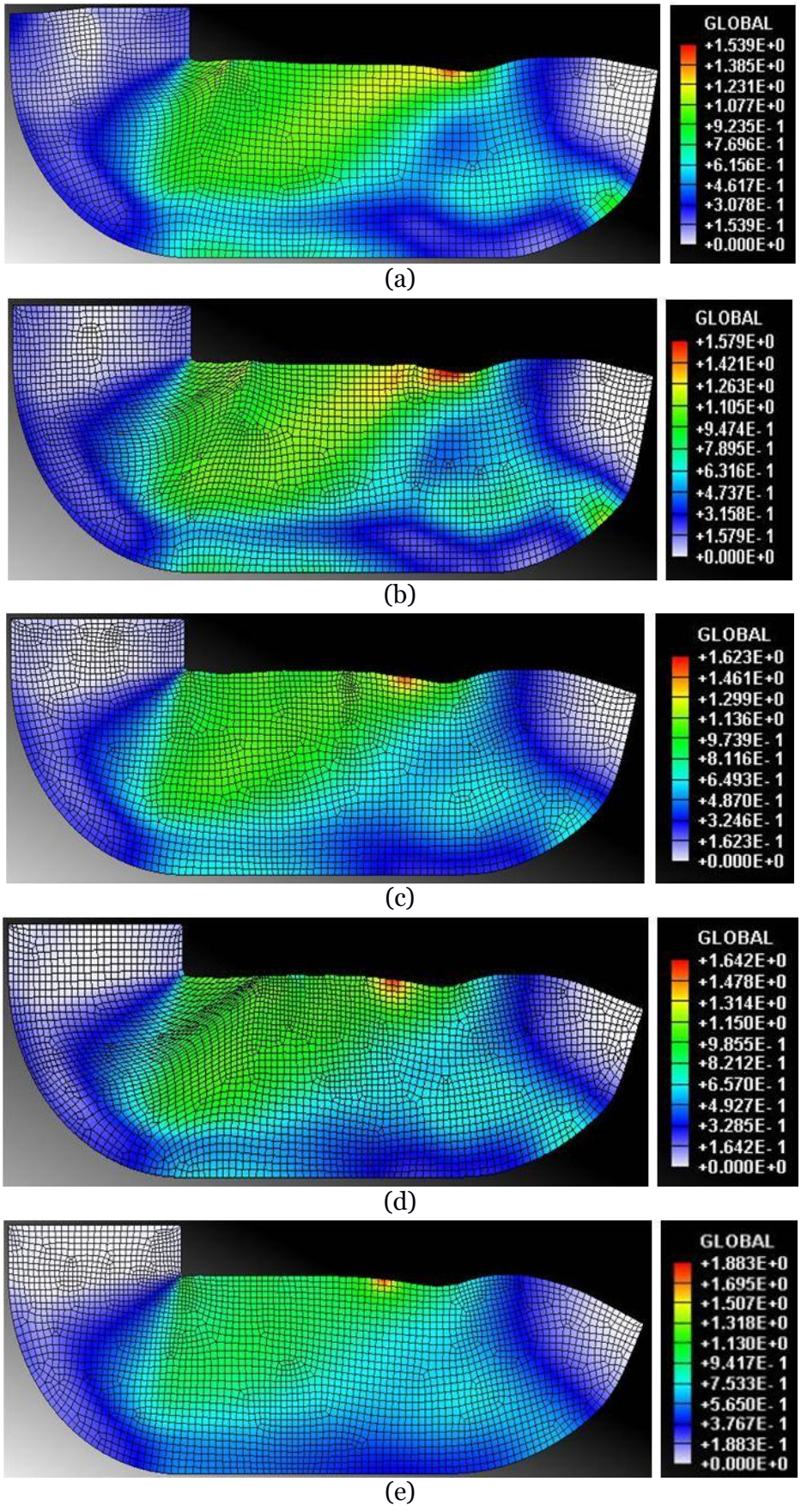

Fig. 6 Effective strain distribution of ECAP process with channel angle 90° having coefficient of friction of (a) 0, (b) 0.1 (c) 0.2 (d) 0.25, (e) and 0.3

Table 3. Results obtained for different values of coefficient of friction for ECAP process

Coefficient of Friction	Effective Strain	Effective Strain Rate (Per Sec.)	Load (tons)
0	1.512	0.9828	0.6
0.1	1.518	1.075	0.8
0.2	1.522	1.241	1
0.25	1.531	1.288	1.1
0.3	1.603	1.308	1.25

ECAP process is also analyzed for die channel angle of 120°, for friction coefficient values of 0, 0.02, 0.06 and 0.1. Fig. 7 shows the effective strain distribution for ECAP process with die channel angle of 120° for varying coefficient friction values, and it is evident that effective strain increases with increase in coefficient of friction values. Strain value of 1.026 is achieved for friction value of 0.1. Fig. 8 gives the clear picture of variation of strain values with respect to varying friction values processed for die corner angle of 120° by ECAP process.

The ECAP process is also simulated for different die corner angles (Ψ), varying from 0° to 90° in the steps of 30°, Fig. 9 shows the effective strain distribution for different die corner angles (Ψ) of ECAP process. It is evident from the results that effective strain value is less for higher corner angles of ECAP process. This is because, at higher value of corner angle allows the material to flow easily without showing much resistance. The highest effective strain recorded is 2.948 for 0° channel angle, while the minimum strain value of 1.531 is achieved with 90° corner angle.

Fig. 10 shows the distribution of effective strain values for two stage ECAP process. Here the comparison between one stage and two stage processing of ECAP is carried out, for die corner angle of 60, 75 and 90 degrees. First the simulation is done for single stage processing for a particular die corner angle, and then the second iteration is carried out by dividing the die corner angle in to two equal halves. It is observed that 2 stage processing of ECAP requires lesser force, compared to single stage processing. But there will be small amount of reduction in effective stain induction in 2 stage ECAP process compare to conventional ECAP process. The effect of stages in ECAP is more, for the acute die corner angle, which is evident in both effective strain distribution and load requirement values.

Fig. 11 shows the load requirement data for different die corner angles, and it can be observed that the gap between both curves decreases as the die corner angle increases. So the selection of feasible die corner angle set will be 60°, 75°, and 90°, considering load requirement data as an important aspect.

Fig. 12 shows the effective strain distribution of the cylindrical tubes, processed by tubular channel angular pressing process, through different die shapes. It can be seen that triangular shaped TCAP imposes more strain compared to trapezoidal shaped TCAP process. But more homogeneous strain distribution is observed in trapezoidal shaped TCAP process compared to triangular shaped TCAP process, i.e. more strain inhomogeneity index (SII) exist in case of to triangular shaped TCAP process. Effective strain of about 1.08 times more is induced in triangular shaped TCAP process in comparison with the trapezoidal shaped TCAP process.

The effective stress distribution of the cylindrical tubes, processed by TCAP process through triangular and trapezoidal shaped dies are plotted in Fig. 13. More homogeneity in stress distribution can be observed in case of trapezoidal shaped TCAP process in comparison with the triangular shaped TCAP process. The Effective stress of about 1.09 times more is induced in triangular shaped TCAP process in comparison with the trapezoidal shaped TCAP process.

Fig. 14 shows the distribution of effective strain rates for triangular and trapezoidal shaped die TCAP processes, the higher magnitude of strain rates are observed in triangular shaped TCAP process in comparison with trapezoidal shaped TCAP process. This is because of

sudden change in geometry of the die in case of triangular shaped TCAP process; this is also one of the reasons for introduction of higher stress and strain values.

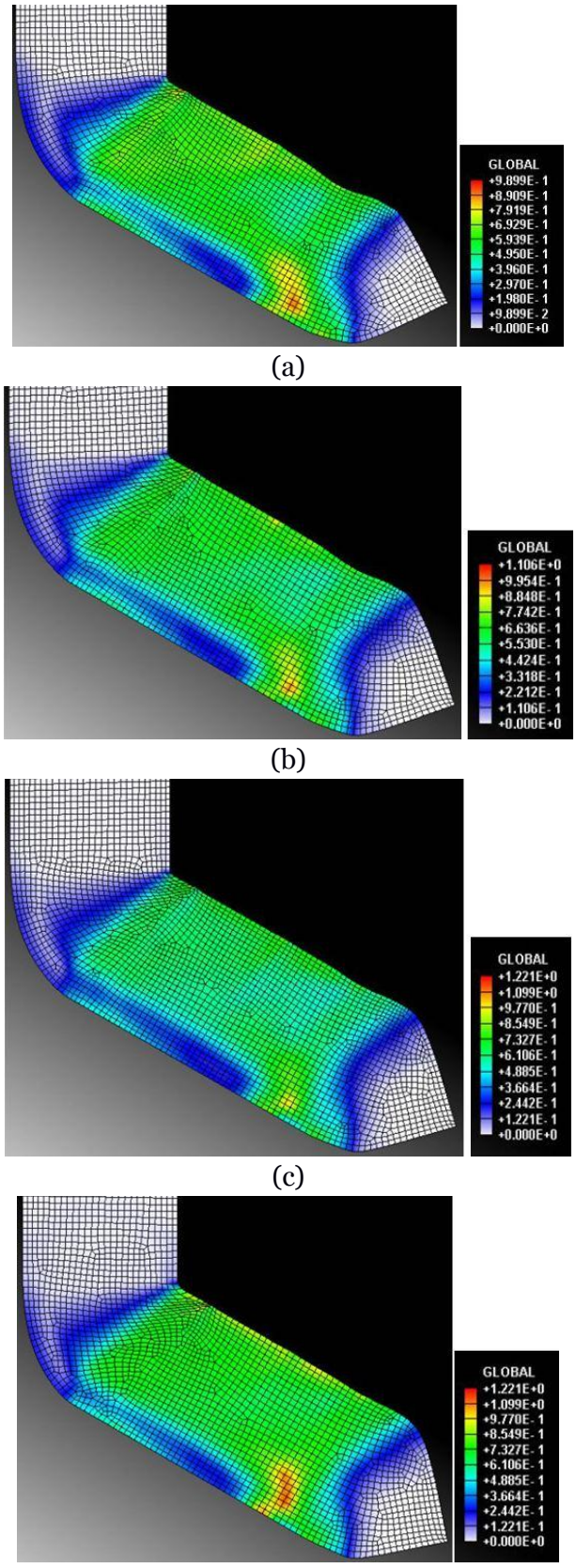

Fig. 7 Effective strain distribution of ECAP with channel angle 120° having coefficient of friction of (a) 0, (b) 0.02 (c) 0.06 and (d) 0.1

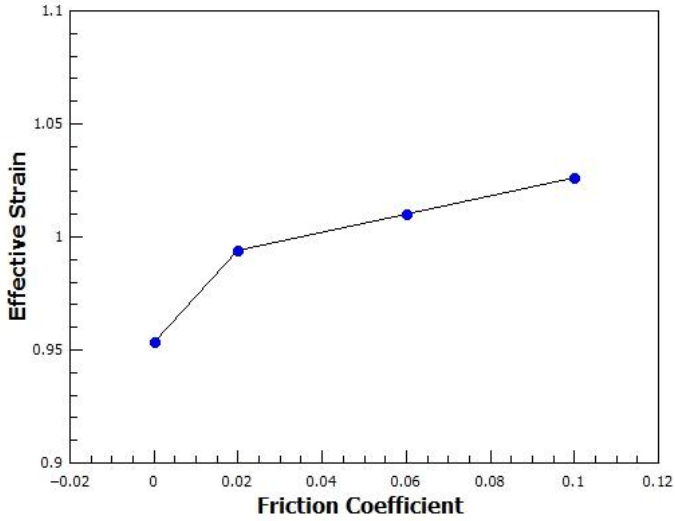

Fig. 8 Effective strain variation during ECAP process for channel angle of 120° versus the friction coefficient

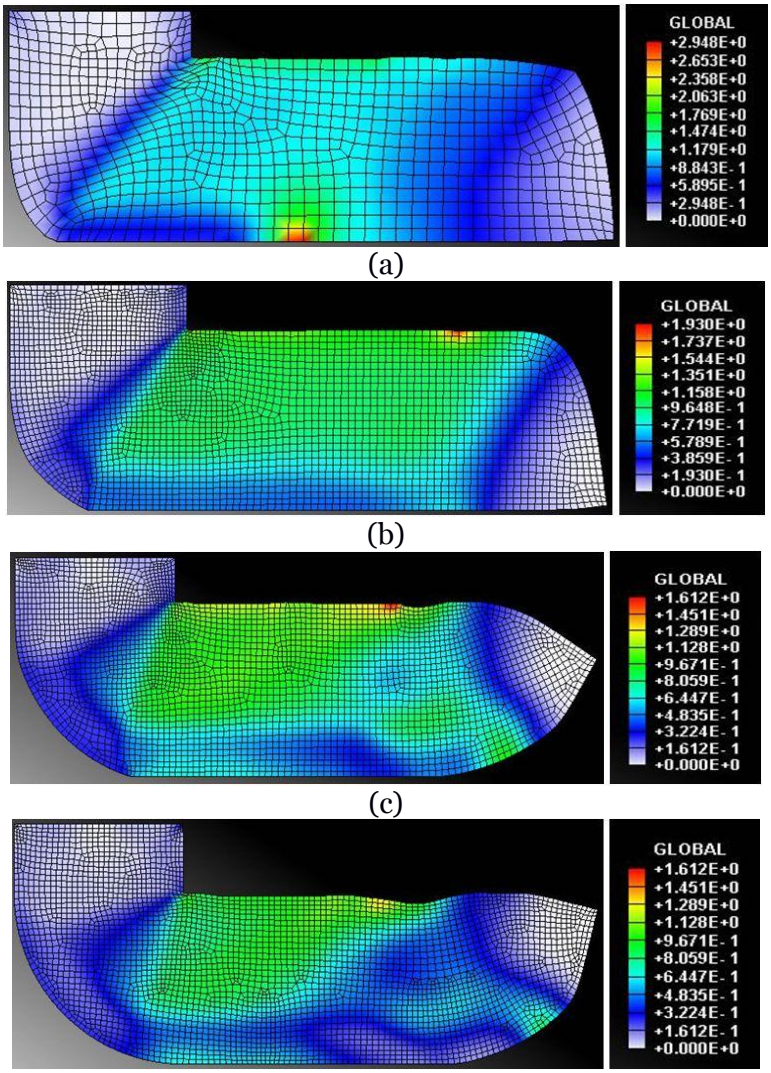

Fig. 9 Effective strain distribution of ECAP process having corner angles (a) 0, (b) 30, (c) 60 and (d) 90 degrees

Maximum effective strain rate of 2.06 is observed in case of triangular shaped TCAP process, while trapezoidal shaped TCAP process induces maximum strain rate of 1.269. TCAP process with trapezoidal shaped die requires only 0.923 times the load and 0.914 times the energy, than the triangular shaped die TCAP process. Detailed results obtained from the analysis are listed in Table 4. The results obtained from FE analysis are compared with the theoretically calculated results for both triangular and trapezoidal shapes TCAP process, and are listed in Table 5. It is evident that FEM results are in good agreement with the theoretical results.
Fig. 15 shows the effective strain distribution of RUE process, which is analyzed for four cycles of RUE process i.e. four set of upsetting and extrusion. The continuous increment in the magnitude of effective strain with increase in number of cycles is observed, and is also plotted in graphical form in Fig. 16. Effective strain distribution is symmetric about the middle plane of the specimen along its vertical axis, and magnitudes of strain are more at the center and lower near the edges. Strain values are minimal at top and bottom of the specimen, this happens because; one side of the material remain undeformed at the end of every stage of the process, depending on the process being carried out. Maximum effective strain of magnitude 3.715 is observed at the end of four cycles of the RUE process.

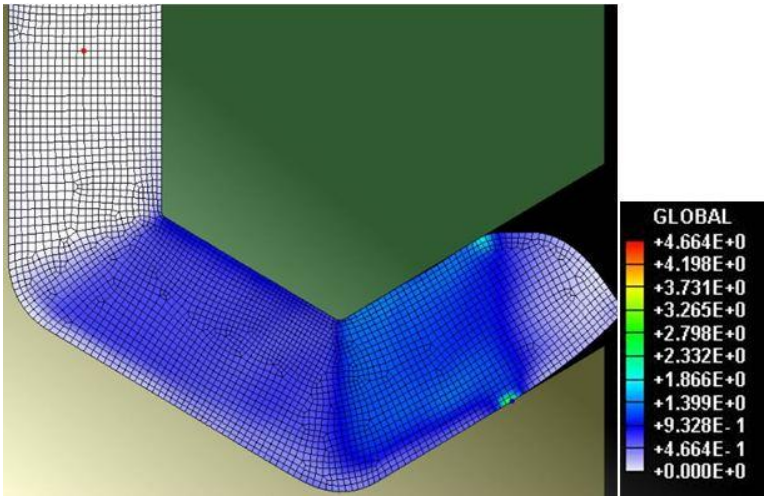

(a)

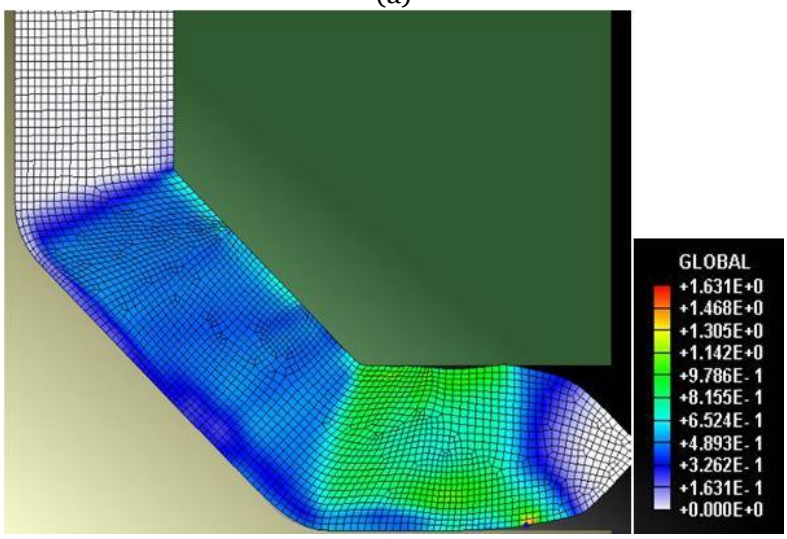

(b)

Fig. 10 Effective strain distribution for two stage ECAP process having channel angles (a) 60/2, and (b) 90/2

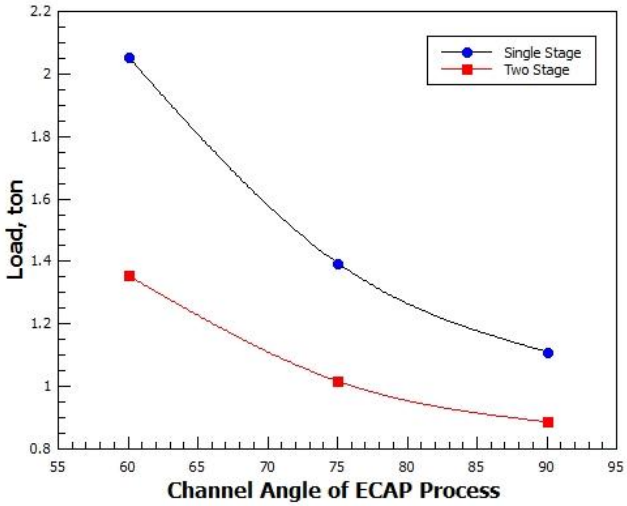

Fig. 11 Load required for ECAP process of different channel angles

Fig. 17 shows the effective stress distribution for RUE process, magnitudes of effective stresses are maximum at the edges, and stress values are minimal at the center of the specimen. Magnitude of effective stress increases continuously with increase in number of cycles, and the variation is also plotted in Fig. 18. When the upsetting and extrusion processes are carried out on the material, they experience shearing across their orientation planes and tend to slide. In Fig. 18 the values of maximum shear stress are also plotted along with effective stress values, it can be seen that maximum shear stress values increase with increase in number of cycles of RUE process. The effective stress of 683.1 MPa is observed at the end of 4 cycles of RUE process. Variation of hydrostatic pressure with respect to number is cycles, is plotted in Fig. 19, where in continuous increment in the values of hydrostatic pressure are observed. Detailed results for all stages of RUE process are listed in Table 6.
Fig. 20 shows the effective strain distribution of CGP process, which is processed for eight stages of CGP. It can be observed that magnitude effective strain increases with increase in number of cycles of CGP process. Homogeneous strain distribution is expected at the end of every 4×n steps, and homogeneity increases with increase in value of n, which is evident from the simulation results. As the value of shear strain is unity, effective strain obtained from defining equation leads to 0.58 and 1.16 at the end of first and second stages of CGP process respectively, and they match with the FEA results obtained from simulations. If four stages are considered as one cycle, then strain homogeneity is highest at fourth stage of every cycle and lowest at the end of second stage. Strain homogeneity for first stage is slightly lesser than the second stage, but more than third stage. Maximum effective strain of 4.1 is observed at the end of eighth stage of CGP process. Strain and homogeneity in strain distribution increases with increasing number of stages.

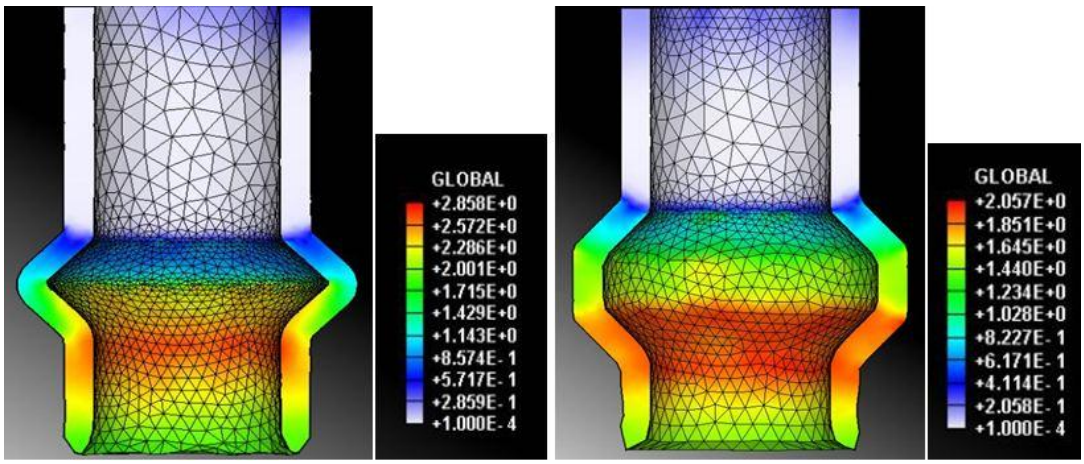

(a) (b)

Fig. 12 Effective strain distribution during TCAP process (a) triangular channel (b) trapezoidal channel

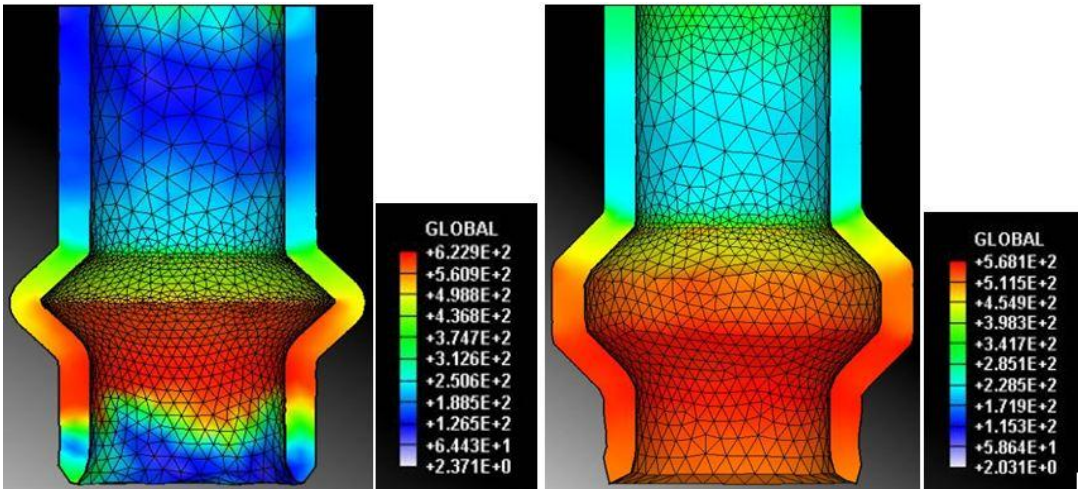

(a) (b)

Fig. 13 Effective stress distribution during TCAP process (a) triangular channel (b) trapezoidal channel

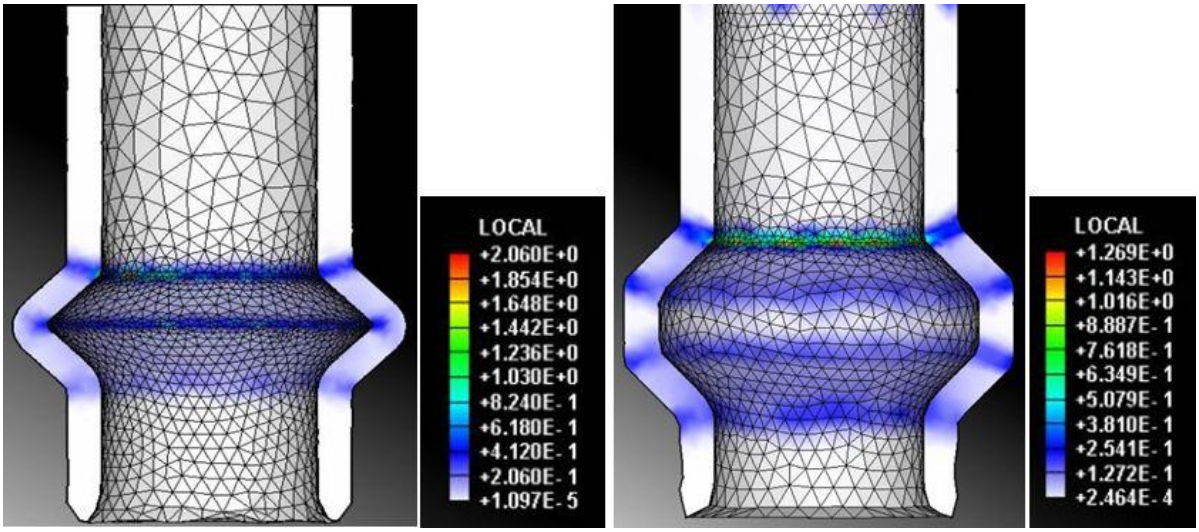

(a) (b)

Fig. 14 Effective strain rate variation during TCAP process (a) triangular channel (b) trapezoidal channel

Table 4. Results obtained for different channels of TCAP process

Channel Shape	Effective Strain	Effective Strain Rate (Per Sec.)	Effective Stress (MPa)	Load (tons)	Energy (J)
Triangular	2.212	2.06	622.9	21.05	206.5
Trapezoidal	2.044	1.269	568.1	19.43	188.8

Table 5. Comparison between FEM and Theoretical effective strain values obtained for TCAP process

Channel Shapes	FEM Results	Theoretical Results
Triangular	2.212	2.86
Trapezoidal	2.044	2.64

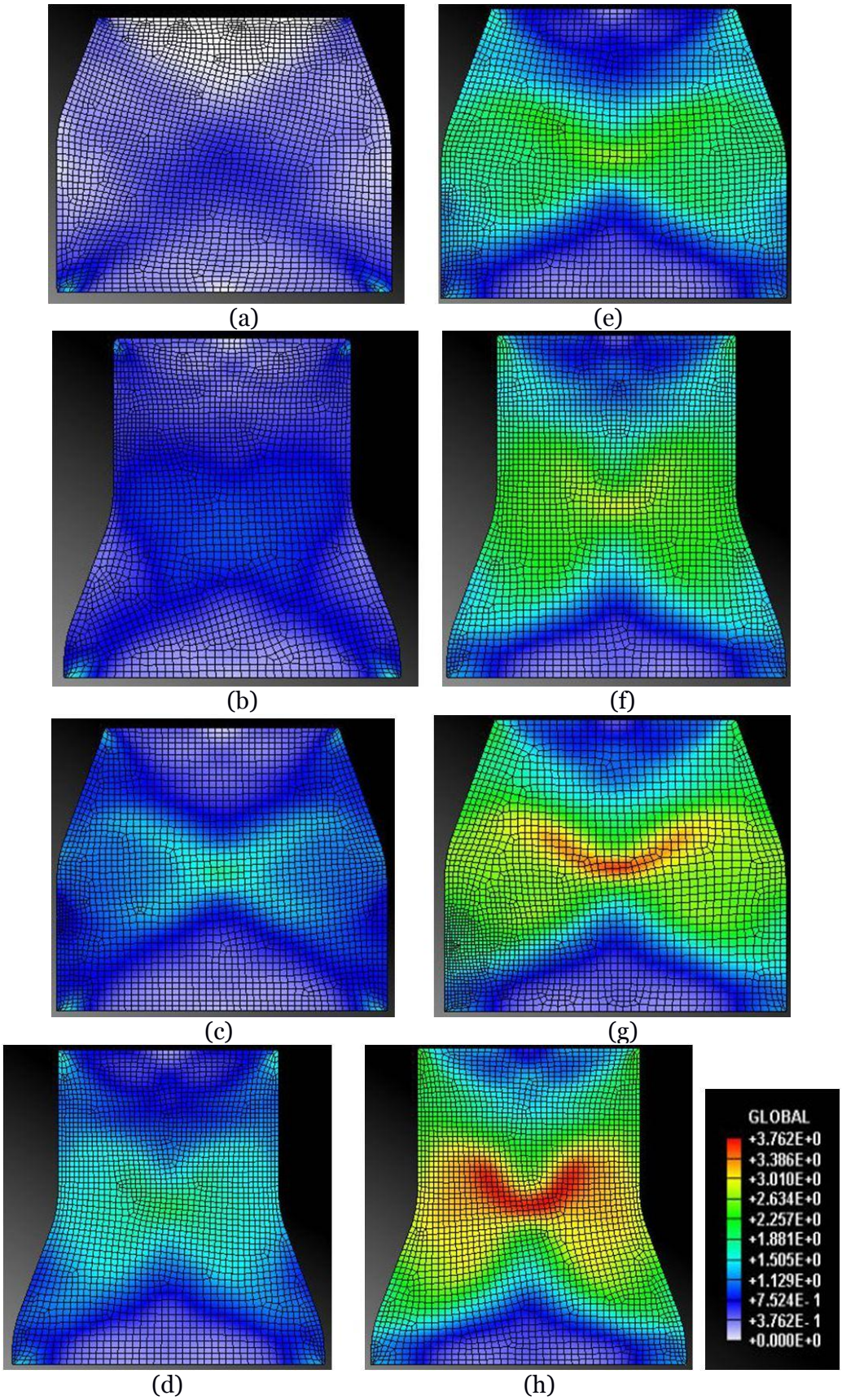

Fig. 15 Effective strain distribution during RUE process for, stage 1 (a) upsetting (b) extrusion, stage 2 (c) upsetting (d) extrusion, stage 3 (e) upsetting (f) extrusion, and stage 4 (g) upsetting (h) extrusion

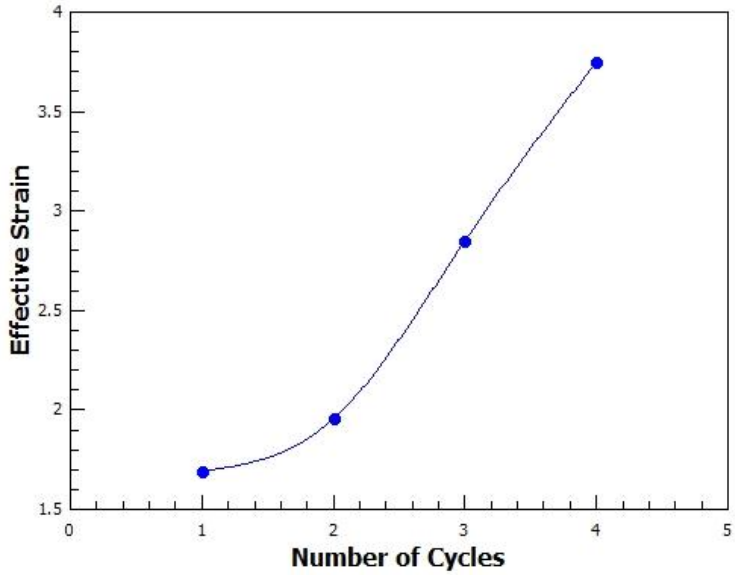

Fig. 16 Variation of effective strain for various number of cycles of RUE process

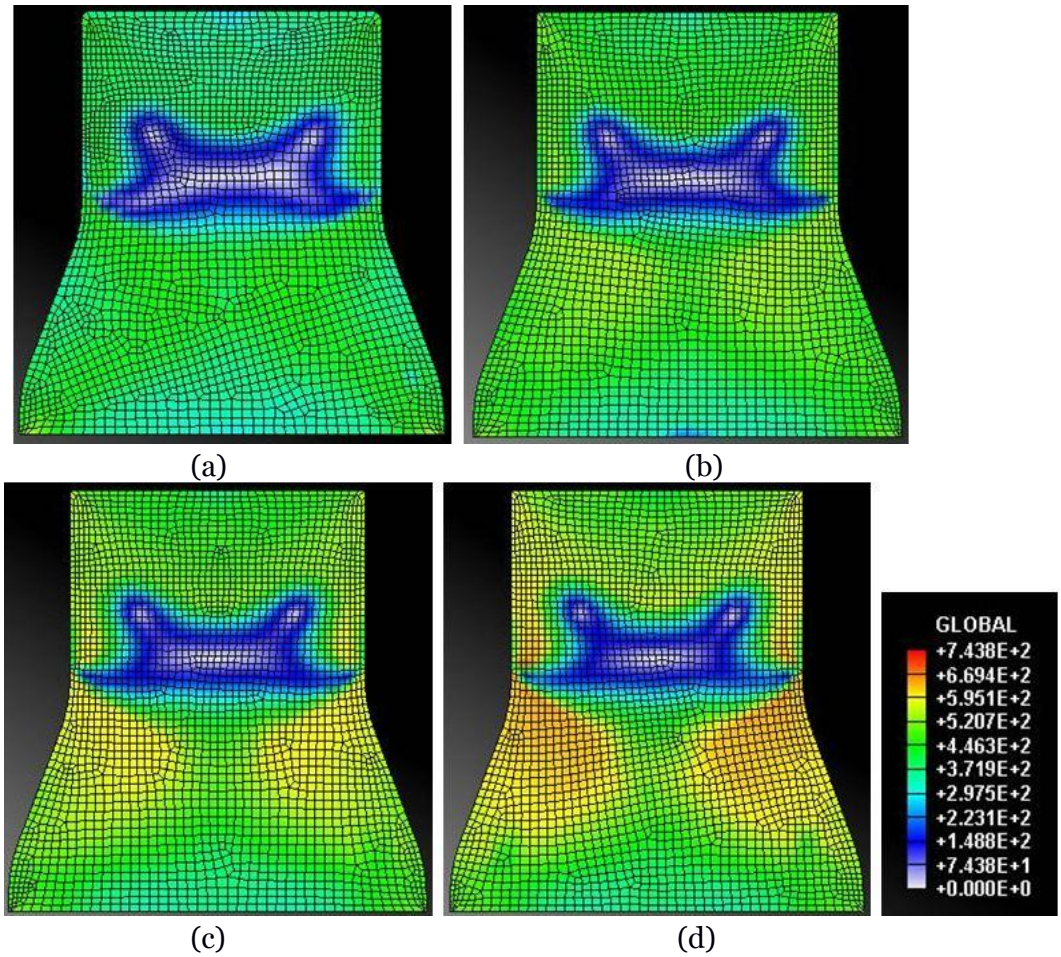

Fig. 17 Effective stress distribution during RUE process at the end of (a) first (b) second, (c) third, and (d) fourth cycles

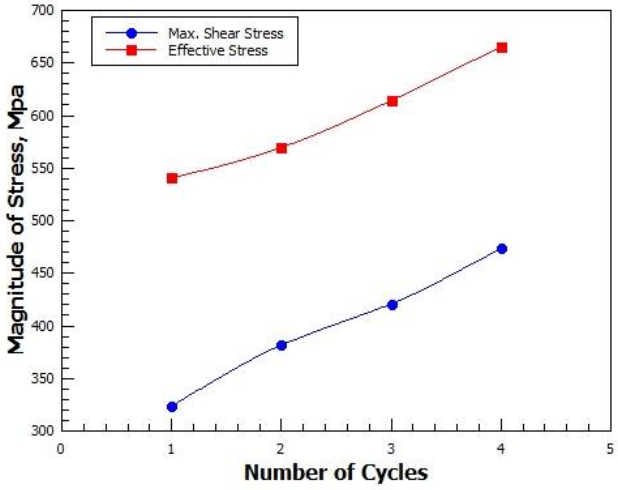

Fig. 18 Variation of effective stress and maximum shear stress for various number of cycles of RUE process

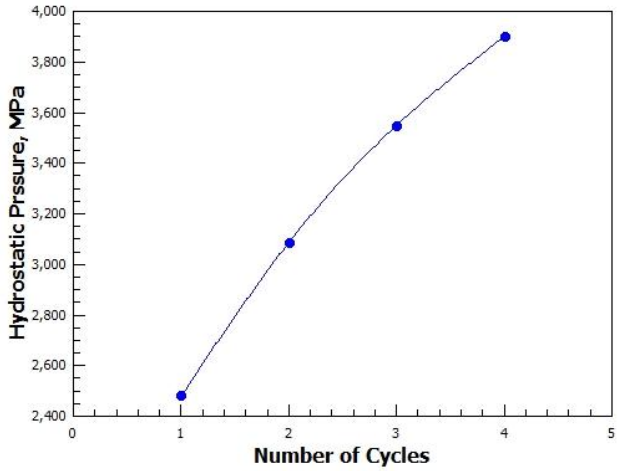

Fig. 19 Variation of hydrostatic pressure for various number of cycles of RUE process

Table 6. Effective strain and effective stress for different stages of RUE process

No of Cycles	Effective Strain	Effective Stress (MPa)
1 Cycle – Upsetting	1.516	535.9
1 Cycle - Extrusion	1.692	540.4
2 Cycle – Upsetting	1.787	553.9
2 Cycle - Extrusion	1.955	569.7
3 Cycle – Upsetting	2.717	614.4
3 Cycle - Extrusion	2.852	629.6
4 Cycle – Upsetting	3.619	665.5
4 Cycle - Extrusion	3.715	683.1

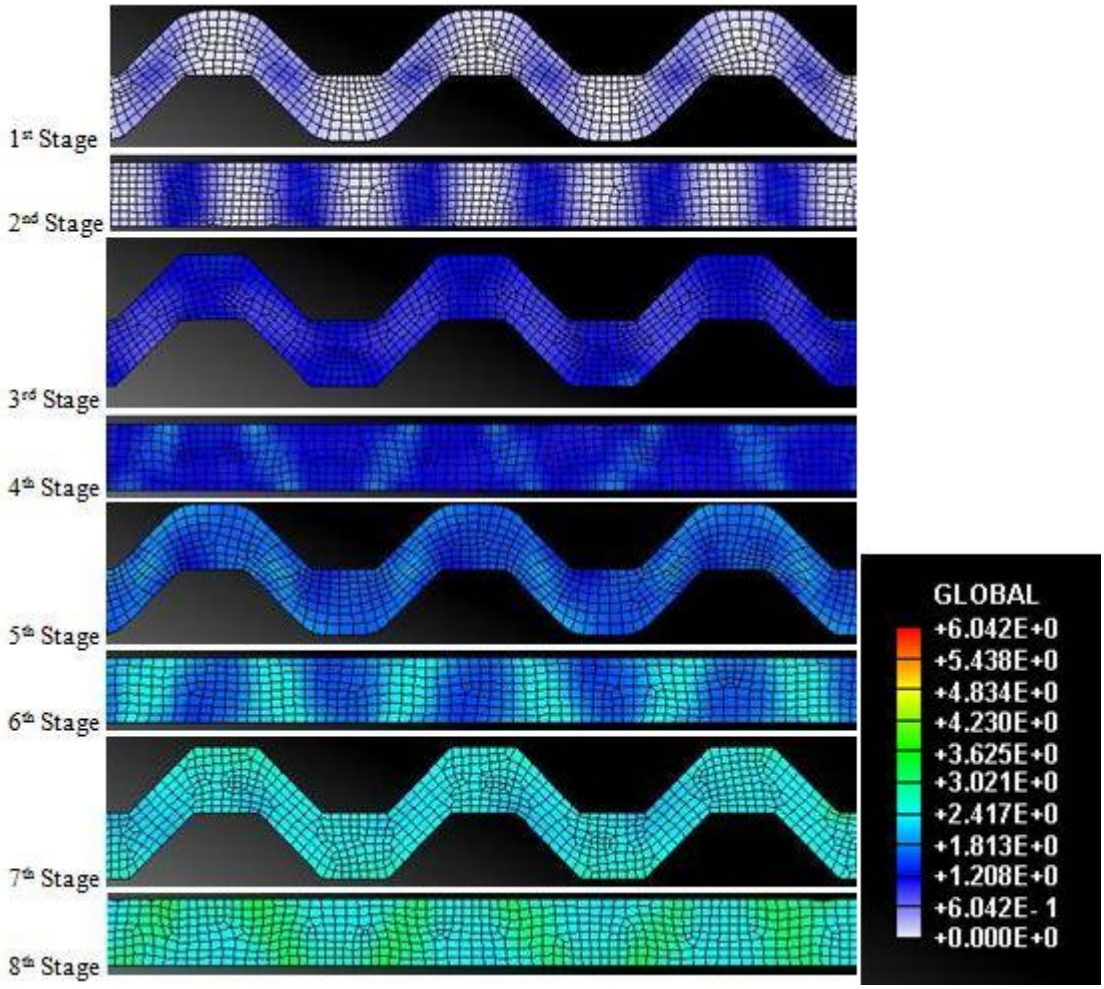

Fig. 20 Effective strain distribution for Aluminum AA- 390 alloy processed by 4 cycles of CGP process

4. Summary and conclusions

1. The finite element analysis for ECAP, TCAP, RUE and CGP processes was carried out successfully. Effect of friction, die corner angle (Ψ) and the channel angle (Φ) on the ECAP process was analyzed; where it was found that effective strain increases up to 1.603 when the friction coefficient was increased to 0.3 with 90° channel angle. For 120° channel angle effective strain reaches up to 1.026 for friction coefficient value of 0.1 .Effective strain of magnitude 2.948 is induced with die corner angle of 0°, which keeps on decreasing with increase in die corner angle. ECAP process was also analyzed for different stages, where it was evident that load required for two stage processing is lesser than the load required for single stage processing, and the effect was more pronounced if the die channel angle is acute.
2. Trapezoidal shaped die TCAP process requires only 0.923 times the load and 0.914 times the energy, as compared to the triangular shaped die TCAP process. TCAP with trapezoidal shaped die achieved homogeneous distribution of both effective strain and effective stress values throughout the specimen.
3. In case of RUE process, effective strain of magnitude 3.715 was induced after 4 cycles, and effective stress of 683.1 MPa was observed at the same stage. In CGP process, it was observed that effective strain distribution was more homogeneous after every 4×n steps, and lowest strain homogeneity was observed in second stage of every CGP cycle.

References

[1] Segal VM, Reznikov VI, Drobyshevkiy AE, Kopylov VI. 1981 *Plastic working of metals by simple shear. (*Russ Metal) p 99-106.
[2] Balasundar M, Sudhakara Rao, T. Raghu, 2009 Equal channel angular pressing die to extrude a variety of materials (*Materials and Design)* p 1050–1059.
[3] M. Shaban Ghazani, A. Vajd, B. Mosadeg, 2014 *Journal of Advanced Materials and Processing*, Vol.2, No. 1, p 47-54.
[4] K. Venkateswarlu, V. Rajinikanth, A.K. Ray, C. Xu and T.G. Langdon, 2010 *Rev. Adv. Mater. Sci. 25* p 99-106.
[5] Basavaraj V Patil, Uday Chakkingal and T S Prasanna Kumar, 2008, *Hradec nad Moravicí,* p 13 –15.
[6] Mohsen E Arai, *MAGNT Research Report (ISSN. 1444-8939)* Vol.2 (2). P: 32-39.
[7] Sanusi KO, Makinde OD, Oliver GJ. *S Afr J Sci.* 2012;108(9/10), Art. #212, 7 pages.
[8] L Olejnik, W Chrominski, A Rosochowski, M Lipinska, M. Lewandowska, 2014 *IOP Conf. Series: Materials Science and Engineering* 63 012004.
[9] Georgy Raab, 2014 *IOP Conf. Series: Materials Science and Engineering* 63 012009.
[10] V.S. Zhernakov, I.N. Budilov, G.I. Raab, I.V. Alexandrov, and R.Z. Valiev, 2001 *Scripta mater.* 44 p 1765–1769.
[11] G. Faraji, M.M. Mashhadi, A.F. Dizadji, M. Hamdi, 2011 *Journal of Mechanical Science and Technology*.
[12] Ghader Faraji, M.M. Mashhadi, Soo-Hyun Joo,and H.S. Kim, 2012 *Rev. Adv. Mater. Sci.* 31 p 12-18.
[13] G. Faraji, F. Reshadi, M. Banisadi, 2014 *Journal of Advanced Matrials and Processing,* Vol.2, No. 1, p 3-12.
[14] I. Balasundar, T. Raghu, 2013 *Int J Mater Form* 6:289-301.
[15] I. Balasundar, K.R. Ravi, T. Raghu, 2013 *Materials Science & Engineering* A 583 p 114-122.
[16] I. Balasundar, T. Raghu, 2013 *Journal of Metallurgical Engineering (ME)* Volume 2 Issue 4.
[17] A. Shirdel, A. Khajeh, M.M. Moshksar, 2010 *Materials and Design* 31 p 946–950.
[18] M. S. Ghazani, A. Vajd, 2014 *Modeling and Numerical Simulation of Material Science*, 4, p 32-36
[19] A. Sajadi, F. Javanroodi, M. Borhani, 2012 *Int J Advanced Design and Manufacturing Technology*, Vol. 5/ No. 2.
[20] N. Solhjoei, A.R. Varposhty, H. Mokhtarian, A. Manian, 2014 *Indian J.Sci.Res.*1(2): 563-572.
[21] Shantharaja M 2013 Mechanical Behaviour of Pure Aluminum Processed by Constrained Groove Pressing. *J Material Sci Eng 2*: 124.
[22] J. Y. Huang, Y. T. Zhu, H. Jiang and T. C. Lowe, 2001 *Acta mater.* 49 p 1497–1505.
[23] H.S. Siddesha and M. Shantharaja 2014 *Procedia Materials Science 5* p 1929 –1936.